

International Conference on Computational Heat and Mass Transfer-2015

## Free Convection of a Nanofluid over an Inclined Wavy Surface Embedded in a Porous Medium with Wall Heat Flux

D. Srinivasacharya\*, P. Vijay Kumar

*Department of Mathematics, National Institute of Technology, Warangal 506 004, India*

### Abstract

The objective of this article is to study the natural convection over an inclined wavy surface embedded in a porous medium saturated with nanofluid. To transform the complex wavy surface to a smooth surface, a coordinate transformation has been used. The governing equations are transformed into a set of partial differential equations using the non-similarity transformations and then applied the local similarity and non-similarity method to obtain ordinary differential equations. These resulting equations are solved using the successive linearization method. The effects of amplitude of the wavy surface, angle of inclination of the wavy surface to the horizontal, Brownian motion parameter, thermophoresis parameter on the non-dimensional heat and nanoparticle mass transfer rates are studied and presented graphically.

© 2015 The Authors. Published by Elsevier Ltd. This is an open access article under the CC BY-NC-ND license (<http://creativecommons.org/licenses/by-nc-nd/4.0/>).

Peer-review under responsibility of the organizing committee of ICCHMT – 2015

**Keywords:** Natural convection; nanofluid; inclined wavy surface; porous medium; heat flux; nanoparticle volume fraction flux

### 1. Introduction

Nanofluids are prepared by suspension of nanometer sized particles in conventional liquids. The term nanofluid was first introduced by Choi [1] to refer this category of fluids. Several researchers have been using nanofluids, so as to attain the highest possible thermal properties at the lowest possible concentrations (preferably < 1% by volume) by stable suspension and uniform dispersion of nanometer sized particles (preferably < 10 nm) in the conventional liquids. The nanoparticles suspended in a conventional liquid are in random motion under the influence of several acting forces, such as the Brownian force. This random motion of the suspended nanoparticles strengthens energy transport inside the liquid. Nanofluids have several engineering applications such as microelectronics, microfluidics, transportation, medicine, solid-state lighting, manufacturing, high-power X-rays, scientific measurement, biomedical, material processing and material synthesis. The detailed review on nanofluids can be found in the book by Das *et al.* [2].

Convective heat and mass transfer in porous media has been widely studied in recent years due to its broad range of engineering applications such as solar energy collectors, heat exchangers, geothermal and hydrocarbon recovery. A

\* Corresponding author. Tel.: +91-9849187249 ; fax: +91-870-2459547.  
E-mail address: [dsc@nitw.ac.in](mailto:dsc@nitw.ac.in)

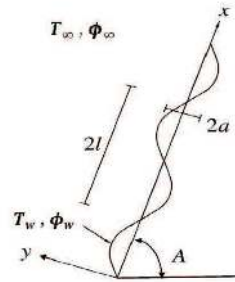


Fig. 1: Physical model

review of convective heat transfer in porous medium is presented in the book by Nield and Bejan [3]. Khan and Aziz [4] numerically investigated the natural convective flow of a nanofluid over a vertical plate with a constant surface heat flux. Haddad *et al.* [5] studied the significance of the effect of Brownian motion and thermophoretic parameters in natural convection of nanofluids. Noghrehabadi *et al.* [6] examined the natural convection heat and mass transfer of nanofluids past a vertical plate under uniform surface heat and nanoparticle mass fluxes in a saturated Darcy porous medium. Thohura *et al.* [7] investigated the problem of steady natural convection along a vertical cone with uniform surface heat flux for temperature dependent thermal conductivity. Chamkha *et al.* [8] studied the effect of uniform heat and nanoparticle fluxes on non-Darcy natural convection of non-Newtonian fluid along a vertical cone embedded in a porous medium filled with nanofluid.

The study of heat and mass transfer from the irregular wavy surfaces is of primary importance because of its enhancing heat transfer characteristics. Tashtoush and Al-Odat [9] numerically investigated the effect of magnetic field on forced convection heat and fluid flow along a wavy surface with prescribed heat flux. Molla *et al.* [10] studied the natural convection boundary layer flow along a vertical complex wavy surface with uniform surface heat flux. Rahman *et al.* [11] studied natural convection flow along a vertical wavy cone with uniform surface heat flux. The preceding literature reveals that the problem of free convection of nanofluid along an inclined wavy surface embedded in a porous medium with uniform surface heat and nanoparticle fluxes has not been considered so far. The present study mainly focused on exploring the effects of amplitude, angle of inclination of the wavy plate to the horizontal, Brownian motion and thermophoresis on natural convection in Darcy porous medium saturated with nanofluid.

## 2. Mathematical Formulation

Consider the steady laminar incompressible two-dimensional boundary layer free convection flow along a semi-infinite inclined wavy surface embedded in a nanofluid saturated porous medium. The wavy plate is inclined at an angle  $A$  ( $0^\circ \leq A \leq 90^\circ$ ) to the horizontal. The inclination angle is  $0^\circ$  (for horizontal plate),  $90^\circ$  (for vertical plate) and  $0^\circ < A < 90^\circ$  (for inclined plate). The coordinate system is shown in Fig. 1. The wavy surface is described by  $y = \delta(x) = a \sin(\pi x/l)$  where  $a$  is the amplitude of the wavy surface and  $2l$  is the characteristic length of the wavy surface. The wavy surface is maintained at uniform heat and nanoparticle volume fraction fluxes. The temperature and nanoparticle volume fraction of the wavy surface are  $T_w$  and  $\phi_w$  respectively and the ambient values of the temperature and nanoparticle volume fraction of the wavy surface are denoted by  $T_\infty$  and  $\phi_\infty$  respectively. The values of  $T_w$  and  $\phi_w$  are assumed to be greater than the ambient temperature  $T_\infty$  and nanoparticle volume fraction  $\phi_\infty$  sufficiently far from the wavy surface.

The porous medium is considered to be homogeneous and isotropic and is saturated with a fluid which is in local thermodynamic equilibrium with the solid matrix. The fluid has constant properties except the density in the buoyancy term of the balance of momentum equation. The governing equations for this problem under the laminar boundary layer flow assumptions, Boussinesq approximation and using the Darcy's flow through a homogeneous porous medium near the inclined wavy surface are given by

$$\frac{\partial u}{\partial x} + \frac{\partial v}{\partial y} = 0 \tag{1}$$

$$\frac{\partial u}{\partial y} - \frac{\partial v}{\partial x} = \frac{(1 - \phi_\infty)\rho_{f\infty}\beta K g}{\mu} \left( \frac{\partial T}{\partial y} \sin A - \frac{\partial T}{\partial x} \cos A \right) - \frac{(\rho_p - \rho_{f\infty})K g}{\mu} \left( \frac{\partial \phi}{\partial y} \sin A - \frac{\partial \phi}{\partial x} \cos A \right) \tag{2}$$

$$u \frac{\partial T}{\partial x} + v \frac{\partial T}{\partial y} = \alpha \left( \frac{\partial^2 T}{\partial x^2} + \frac{\partial^2 T}{\partial y^2} \right) + \gamma \left[ D_B \left( \frac{\partial \phi}{\partial x} \frac{\partial T}{\partial x} + \frac{\partial \phi}{\partial y} \frac{\partial T}{\partial y} \right) + \frac{D_T}{T_\infty} \left( \left( \frac{\partial T}{\partial x} \right)^2 + \left( \frac{\partial T}{\partial y} \right)^2 \right) \right] \tag{3}$$

$$u \frac{\partial \phi}{\partial x} + v \frac{\partial \phi}{\partial y} = D_B \left( \frac{\partial^2 \phi}{\partial x^2} + \frac{\partial^2 \phi}{\partial y^2} \right) + \frac{D_T}{T_\infty} \left( \frac{\partial^2 T}{\partial x^2} + \frac{\partial^2 T}{\partial y^2} \right) \tag{4}$$

where  $u$  and  $v$  are the Darcy velocity components in the  $x$  and  $y$  directions respectively,  $T$  is the temperature,  $\phi$  is the nanoparticle concentration,  $g$  is the acceleration due to gravity,  $K$  is the permeability,  $\rho_f$  is the the density of the base fluid,  $\rho_p$  is the density of the particles,  $\alpha$  is the effective thermal diffusivity,  $\beta$  is the volumetric thermal expansion coefficient of the nanofluid,  $\mu$  is the dynamic viscosity of the fluid,  $D_B$  is the Brownian diffusion coefficient,  $D_T$  is the thermophoretic diffusion coefficient and  $\gamma$  is the ratio between the effective heat capacity of the nanoparticle material and heat capacity of the fluid.

The boundary conditions are

$$v = 0, \quad q_w = -k(n \cdot \nabla T), \quad q_{np} = D_B(n \cdot \nabla \phi), \quad \text{at } y = \delta(x) \tag{5a}$$

$$u = 0, \quad T \rightarrow T_\infty, \quad \phi \rightarrow \phi_\infty \quad \text{as } y \rightarrow \infty \tag{5b}$$

Introducing the stream function  $\psi$  by  $u = \frac{\partial \psi}{\partial y}$ ,  $v = -\frac{\partial \psi}{\partial x}$  and the following non-dimensional variables

$$\xi = x/l, \quad \eta = \frac{(y/l - \delta) Ra^{1/3}}{\xi^{1/3} (1 + \delta^2)}, \quad \psi = \alpha Ra^{1/3} \xi^{2/3} f(\xi, \eta), \quad T - T_\infty = \frac{q_w l}{k} \xi^{1/3} Ra^{-1/3} \theta(\xi, \eta),$$

$$\phi - \phi_\infty = \frac{q_{np} l}{D_B} \xi^{1/3} Ra^{-1/3} s(\xi, \eta), \tag{6}$$

into Eqs.(1)-(4) and letting  $Ra \rightarrow \infty$  (i.e., boundary layer approximation), we obtain the following boundary layer equations:

$$f'' = (\sin A + \delta \cos A) (\theta' - N_r s') \tag{7}$$

$$\theta'' + \frac{2}{3} f \theta' - \frac{1}{3} f' \theta + \xi^{1/3} N_b s' \theta' + \xi^{1/3} N_t \theta'^2 = \xi \left( f' \frac{\partial \theta}{\partial \xi} - \theta' \frac{\partial f}{\partial \xi} \right) \tag{8}$$

$$s'' + \frac{2}{3} Le f s' - \frac{1}{3} Le f' s + \frac{N_t}{N_b} \theta'' = Le \xi \left( f' \frac{\partial s}{\partial \xi} - s' \frac{\partial f}{\partial \xi} \right) \tag{9}$$

The associated boundary conditions are

$$2f + 3\xi \left( \frac{\partial f}{\partial \xi} \right)_{\eta=0} = 0, \quad \theta' = -\sqrt{1 + \delta^2}, \quad s' = -\sqrt{1 + \delta^2}, \quad \text{at } \eta = 0 \tag{10a}$$

$$f' = 0, \quad \theta \rightarrow 0, \quad s \rightarrow 0 \quad \text{as } \eta \rightarrow \infty, \tag{10b}$$

where  $Ra = \frac{(1 - \phi_\infty)\rho_{f\infty}\beta K g q_w l^2}{\mu k \alpha}$  is the Rayleigh number,  $N_r = \frac{(\rho_p - \rho_{f\infty})k q_{np}}{(1 - \phi_\infty)\rho_{f\infty}\beta q_w D_B}$  is the buoyancy ratio,  $N_b = \frac{\gamma q_{np} l}{\alpha} Ra^{-1/3}$  is the Brownian motion parameter,  $N_t = \frac{\gamma D_T q_w l}{\alpha T_\infty k} Ra^{-1/3}$  is the thermophoresis parameter and  $Le = \frac{\alpha}{D_B}$  is the Lewis number.

The local Nusselt number  $Nu_\xi$  and the nanoparticle Sherwood number  $NSh_\xi$  are the parameters of engineering interest. These parameters characterize the wall heat and nanoparticle mass transfer rates, respectively.

The dimensionless local Nusselt number  $Nu_\xi = \frac{xq_w}{k(T_w - T_\infty)}$  and the nanoparticle Sherwood number  $NSh_\xi = \frac{xq_{np}}{D_B(\phi_w - \phi_\infty)}$  are given by

$$\frac{Nu_\xi}{Ra_\xi^{1/3}} = \frac{\xi^{1/3}}{\theta(\xi, 0)}, \quad \frac{NSh_\xi}{Ra_\xi^{1/3}} = \frac{\xi^{1/3}}{s(\xi, 0)} \tag{11}$$

### 3. Method of Solution

To solve the system of Eqns. (7)-(9) along with the boundary conditions (10), a local similarity and non-similarity method [12,13] has been applied. The boundary value problems obtained from this method are solved by the successive linearisation method.

In the first level of truncation, the terms accompanied by  $\xi \frac{\partial}{\partial \xi}$  are assumed to be very small. This is particularly true when  $\xi \ll 1$ . Thus the terms with  $\xi \frac{\partial}{\partial \xi}$  in Eqns. (7)-(9) can be neglected to get the following system of equations.

$$f'' = (\sin A + \delta \cos A) (\theta' - N_r s') \tag{12}$$

$$\theta'' + \frac{2}{3} f \theta' - \frac{1}{3} f' \theta + \xi^{1/3} N_b s' \theta' + \xi^{1/3} N_t \theta'^2 = 0 \tag{13}$$

$$s'' + \frac{2}{3} Le f s' - \frac{1}{3} Le f' s + \frac{N_t}{N_b} \theta'' = 0 \tag{14}$$

The associated boundary conditions are

$$f = 0, \quad \theta' = -\sqrt{1 + \delta^2}, \quad s' = -\sqrt{1 + \delta^2} \quad \eta = 0 \tag{15a}$$

$$f' = 0, \quad \theta \rightarrow 0, \quad s \rightarrow 0 \quad \text{as } \eta \rightarrow \infty, \tag{15b}$$

For the second level of truncation we introduce  $g = \frac{\partial f}{\partial \xi}$ ,  $h = \frac{\partial \theta}{\partial \xi}$  and  $k = \frac{\partial s}{\partial \xi}$  and recover the neglected terms at the first level of truncation. Thus the governing equations at the second level reduces to

$$f'' = (\sin A + \delta \cos A) (\theta' - N_r s') \tag{16}$$

$$\theta'' + \frac{2}{3} f \theta' - \frac{1}{3} f' \theta + \xi^{1/3} N_b s' \theta' + \xi^{1/3} N_t \theta'^2 = \xi (f' h - \theta' g) \tag{17}$$

$$s'' + \frac{2}{3} Le f s' - \frac{1}{3} Le f' s + \frac{N_t}{N_b} \theta'' = Le \xi (f' k - s' g) \tag{18}$$

The associated boundary conditions are

$$2f + 3\xi g = 0, \quad \theta' = -\sqrt{1 + \delta^2}, \quad s' = -\sqrt{1 + \delta^2} \quad \eta = 0 \tag{19a}$$

$$f' = 0, \quad \theta \rightarrow 0, \quad s \rightarrow 0 \quad \text{as } \eta \rightarrow \infty, \tag{19b}$$

At the third level of truncation we differentiate Eqns. (16) - (19) with respect to  $\xi$  and neglect the terms  $\frac{\partial g}{\partial \xi}$ ,  $\frac{\partial h}{\partial \xi}$  and  $\frac{\partial k}{\partial \xi}$  to get the following system of equations

$$g'' = (\delta \cos A) (\theta' - N_r s') + (\sin A + \delta \cos A) (h' - N_r k') \tag{20}$$

$$h'' + \frac{5}{3} g \theta' + \frac{2}{3} f h' - \frac{1}{3} g' \theta - \frac{4}{3} f' h + \frac{1}{3} N_b \xi^{-2/3} s' \theta' + N_b \xi^{1/3} (k' \theta' + s' h') + \frac{1}{3} N_t \xi^{-2/3} \theta'^2 + 2N_t \xi^{1/3} \theta' h' - \xi (g' h - h' g) = 0 \tag{21}$$

$$k'' + \frac{5}{3}Legs' + \frac{2}{3}Lefk' - \frac{1}{3}Leg's - \frac{4}{3}Le f'k + \frac{N_l}{N_b}h'' - Le\xi(g'k - k'g) = 0 \tag{22}$$

The associated boundary conditions are

$$g = 0, \quad h' = -\frac{\delta\delta}{\sqrt{1+\delta^2}}, \quad k' = -\frac{\delta\delta}{\sqrt{1+\delta^2}}, \quad \text{at } \eta = 0 \tag{23a}$$

$$g' = 0, \quad h \rightarrow 0, \quad k \rightarrow 0 \quad \text{as } \eta \rightarrow \infty, \tag{23b}$$

The set of differential equations (16) - (18) and (20) - (22) together with the boundary conditions (19) and (23) are solved using successive linearisation method([14,15]). Using this method the non linear boundary layer equations reduce to a system of linear differential equations. The Chebyshev pseudo spectral method is then used to transform the iterative sequence of linearized differential equations into a system of linear algebraic equations which are converted into a matrix system.

Let  $\mathbf{Y}(\eta) = [f(\eta), \theta(\eta), s(\eta), g(\eta), h(\eta), k(\eta)]$  and assume that the independent vector  $\mathbf{Y}(\eta)$  can be expressed as

$$\mathbf{Y}(\eta) = \mathbf{Y}_i(\eta) + \sum_{n=0}^{i-1} \mathbf{Y}_n(\eta) \tag{24}$$

where  $\mathbf{Y}_i(\eta)$ , ( $i = 1, 2, 3, \dots$ ) are unknown vectors and  $\mathbf{Y}_n(\eta)$  are the approximations which are obtained by recursively solving the linear part of the equation system that results from substituting (24) in (16)-(23).

The initial approximations are chosen such that they satisfy the boundary conditions (19) and (23). The subsequent solutions  $f_i, \theta_i, s_i, g_i, h_i$ , and  $k_i, i \geq 1$  are obtained by successively solving the linearized form of the equations which are obtained by substituting Eq.(24) in the governing equations.

The approximate solutions for  $\mathbf{Y}(\eta)$  are then obtained as  $\mathbf{Y}(\eta) \approx \sum_{m=0}^M \mathbf{Y}_m(\eta)$  where  $M$  is the order of SLM approximation. The linearized equations are solved using the Chebyshev spectral collocation method [16]. The unknown functions are approximated by the Chebyshev interpolating polynomials in such a way that they are collocated at the Gauss-Lobatto points defined as

$$\xi_j = \cos \frac{\pi j}{N}, \quad j = 0, 1, 2, \dots, N \tag{25}$$

where  $N$  is the number of collocation points used. The physical region  $[0, \infty)$  is transformed into the region  $[-1, 1]$  using the domain truncation technique in which the problem is solved on the interval  $[0, L]$  instead of  $[0, \infty)$ . This leads to the mapping

$$\frac{\eta}{L} = \frac{\xi + 1}{2}, \quad -1 \leq \xi \leq 1 \tag{26}$$

where  $L$  is a scaling parameter used to invoke the boundary condition at infinity. The function  $\mathbf{Y}(\eta)$  is approximated at the collocation points by

$$\mathbf{Y}_i(\xi) = \sum_{k=0}^N \mathbf{Y}_i(\xi_k)T_k(\xi_j), \quad j = 0, 1, 2, \dots, N \tag{27}$$

where  $T_k$  is the  $k^{th}$  Chebyshev polynomial defined by  $T_k(\xi) = \cos[k\cos^{-1}\xi]$ . The derivatives of the variables at the collocation points are represented as

$$\frac{d^a}{d\eta^a} \mathbf{Y}_i(\xi) = \sum_{k=0}^N \mathbf{D}_{kj}^a \mathbf{Y}_i(\xi_k), \quad j = 0, 1, 2, \dots, N. \tag{28}$$

where  $a$  is the order of differentiation and  $\mathbf{D} = \frac{2}{L} \mathcal{D}$  with  $\mathcal{D}$  being the Chebyshev spectral differentiation matrix. Substituting Eqs.(26)-(28) into linearized form of equations leads to the matrix equation

$$\mathbf{A}_{i-1} \mathbf{X}_i = \mathbf{R}_{i-1}, \tag{29}$$

In Eq.(29),  $\mathbf{A}_{i-1}$  is a  $(6N + 6) \times (6N + 6)$  square matrix and  $\mathbf{X}_i$  and  $\mathbf{R}_{i-1}$  are  $(6N + 6) \times 1$  column vectors defined by

$$\mathbf{A}_{i-1} = [A_{pq}], \quad p, q = 1, 2, \dots, 6 \quad \mathbf{X}_i = [\mathbf{F}_i, \boldsymbol{\Theta}_i, \boldsymbol{\Phi}_i, \mathbf{G}_i, \mathbf{H}_i, \mathbf{K}_i]^T, \quad \mathbf{R}_{i-1} = [\mathbf{r}_{1,i-1}, \mathbf{r}_{2,i-1}, \mathbf{r}_{3,i-1}, \mathbf{r}_{4,i-1}, \mathbf{r}_{5,i-1}, \mathbf{r}_{6,i-1}]^T \tag{30}$$

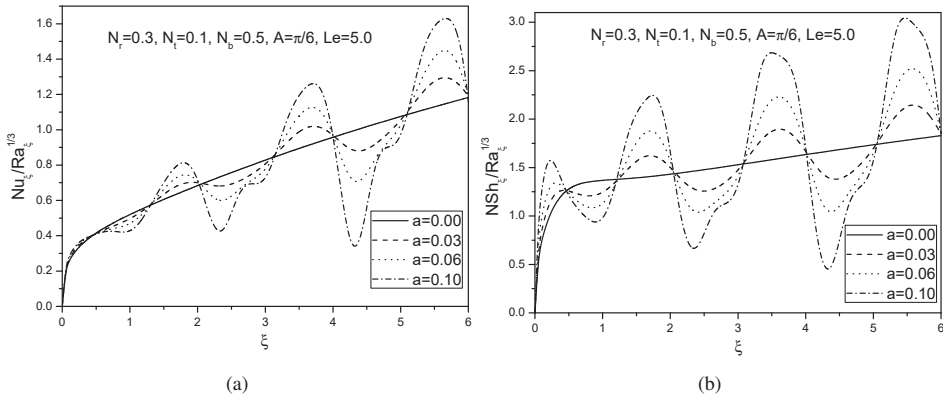


Fig. 2: Effect of the wave amplitude  $a$  on the heat and nanoparticle mass transfer rates.

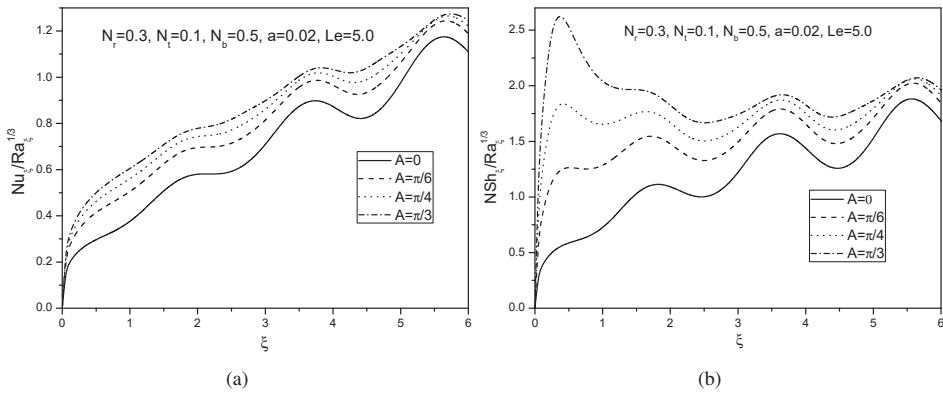


Fig. 3: Effect of the Angle of inclination ( $A$ ) on the heat and nanoparticle mass transfer rates.

Where  $a_{k,i-1}, b_{k,i-1}, c_{k,i-1}, d_{k,i-1}, l_{k,i-1}, m_{k,i-1}$  are diagonal matrices of size  $(N+1) \times (N+1)$  and  $I$  is an identity matrix of size  $(N+1) \times (N+1)$ . After modifying the matrix system (29) to incorporate boundary conditions, the solution is obtained as

$$\mathbf{X}_i = \mathbf{A}_{i-1}^{-1} \mathbf{R}_{i-1} \tag{31}$$

#### 4. Results and Discussion

The solutions for dimensionless heat and nanoparticle mass transfer rates are computed and presented graphically in Figs. 2-5. The effects of angle of inclination ( $A$ ), Brownian motion parameter ( $N_b$ ), thermophoresis parameter ( $N_t$ ) and amplitude ( $a$ ) of the wavy surface have been discussed.

The effect of the wave amplitude on the Nusselt and nanoparticle Sherwood number is plotted in Fig. 2. This figure shows that an enhancement in wavy amplitude increases the local heat and nanoparticle mass transfer rates as compared with the limiting case of a smooth surface. Hence, the Streamwise distribution of the local Nusselt and nanoparticle Sherwood number are harmonic curves with wavelength is equal to the wavelength of the inclined wavy surface ( $0^\circ < A < 90^\circ$ ). But, the Streamwise distribution of the local Nusselt and nanoparticle Sherwood number are harmonic curves with wavelength is equal to twice the wavelength of the vertical wavy surface ( $A = 90^\circ$ ). In general, we conclude that the surface becomes more roughened for increasing values of amplitude of the wavy surface.

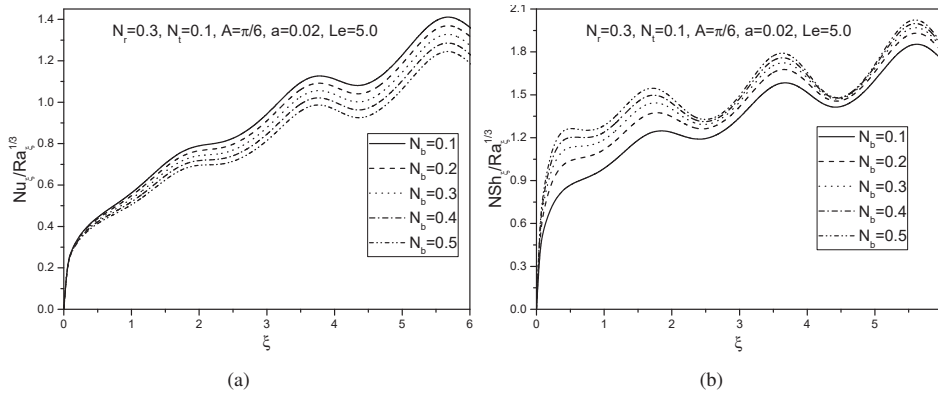


Fig. 4: Effect of the Brownian motion parameter ( $N_b$ ) on the heat and nanoparticle mass transfer rates.

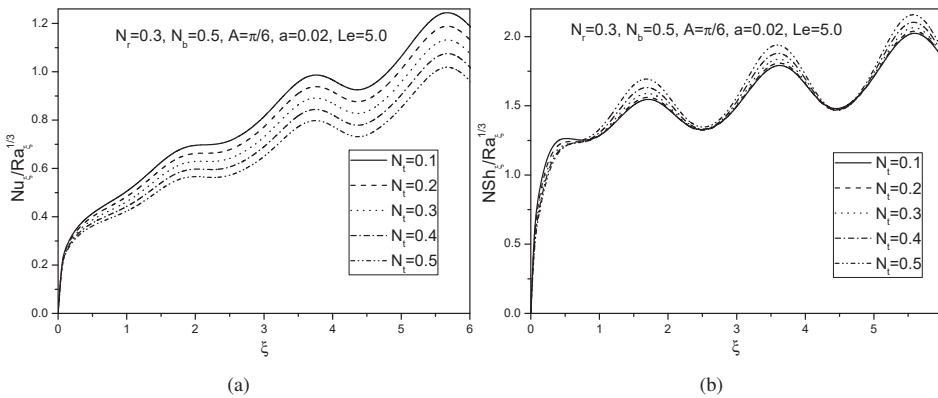


Fig. 5: Effect of the thermophoresis parameter ( $N_t$ ) on the heat and nanoparticle mass transfer rates.

The variation of heat and nanoparticle mass transfer rates for various values of the angle of inclination  $A$  is displayed in Fig. 3. This figure shows that increasing the angle of inclination increases the buoyancy force and assist the flow, leading to an increase in the heat and nanoparticle mass transfer rates. The maximum values of the dimensionless heat and nanoparticle mass transfer rates are observed when the surface is vertical; in which case, the buoyancy force is at its maximum.

The effect of Brownian motion parameter  $N_b$  on the heat and nanoparticle mass transfer rates is presented in Fig. 4. Fig. 4(a) depicts that the dimensionless heat transfer rate decreases with the increase in the Brownian motion parameter. An increase in the value of Brownian motion parameter enhances the nanoparticle volume fraction transfer rate, as shown in Fig. 4(b)

Fig. 5 depicts the streamwise distribution of Nusselt and Sherwood numbers for different values of thermophoresis parameter  $N_t$ . It is seen from Fig. 5(a) that the heat transfer rate decreases with the increase in the thermophoresis parameter. The effect of thermophoresis number on nanoparticle mass transfer is to increase the nanoparticle Sherwood number as depicted in Fig. 5(b).

**5. Conclusions**

The problem of free convection heat and mass transfer over an inclined wavy surface embedded in a porous medium saturated with nanofluid with uniform surface heat and nanoparticle volume fraction fluxes was analyzed. Numerical

solutions were obtained for different values of Brownian motion parameter, thermophoresis parameter, amplitude and angle of inclination of the wavy surface. The Brownian motion parameter  $N_b$  significantly affects flow field i.e. increasing the Brownian motion parameter increases the nanoparticle mass transfer rate but reduces the heat transfer of the fluid. The effect of the thermophoresis parameter  $N_t$ , on the fluid flow is to increase the local nanoparticle mass transfer coefficient and to decrease the local heat transfer coefficient. An increase in the value of the wavy amplitude  $a$  enhances the local heat and nanoparticle mass transfer rates of the fluid. The effect of angle of inclination  $A$  of the wavy surface was found to enhance the heat and nanoparticle mass transfer rates of the fluid.

## References

- [1] S. U. S. Choi, J. A. Eastman, Enhancing thermal conductivity of fluids with Nanoparticles, Developments and applications of Non-Newtonian flows, ASME MD. 231 (1995) 99-105.
- [2] S. K. Das, S. U. S. Choi, W. Yu, T. Pradeep, Nanofluids: Science and Technology, Wiley Interscience, New Jersey (2007).
- [3] D. A. Nield, A. Bejan, Convection in Porous Media, 4th ed., Springer, New York (2013).
- [4] W. A. Khan, A. Aziz, Natural convection flow of a nanofluid over a vertical plate with uniform surface heat flux, Int. J. Thermal Sciences. 50 (2011) 1207-1214.
- [5] Z. Haddad, E. Abu-Nada, H. F. Oztop, A. Mataoui, Natural convection in nanofluids: Are the thermophoresis and Brownian motion effects significant in nanofluid heat transfer enhancement, Int. J. Thermal Sciences. 57 (2012) 152-162.
- [6] A. Noghrehabadi, A. Behseresht, M. Ghalambaz, Natural convection of nanofluid over vertical plate embedded in porous medium: prescribed surface heat flux, Appl. Math. Mech. -Engl. Ed. 34 (2013) 669-686.
- [7] S. Thohura, A. Rahman, M. M. Molla, M. M. A. Sarker, Effects of temperature dependent thermal conductivity on natural convection flow along a vertical wavy cone with heat flux, Procedia Engineering 90 (2014) 497-503.
- [8] A. J. Chamkha, S. Abbasbandy, A. M. Rashad, Non-Darcy natural convective flow for non-Newtonian nanofluid over a cone saturated in porous medium with uniform heat and volume fraction fluxes, Int. J. Numerical Methods for Heat and Fluid Flow. 25 (2015) 422-437.
- [9] B. Tashtoush, M. Al-Odat, Magnetic field effect on heat and fluid flow over a wavy surface with a variable heat flux, Journal of Magnetism and Magnetic Materials. 268 (2004) 357-363.
- [10] M. Molla, A. Hossain, L. S. yao, Natural convection flow along a vertical complex wavy surface with uniform surface heat flux, ASME J. Heat Transfer. 129 (2007) 1403-1407.
- [11] A. Rahman, M. M. Molla, M. M. A. Sarker, Natural convection flow along the vertical wavy cone in case of uniform surface heat flux where viscosity is an exponential function of temperature, Int. Comm. Heat Mass Transfer 38 (2011) 774-780.
- [12] W. J. Minkowycz, E. M. Sparrow, Local non-similar solution for natural convection on a vertical cylinder, ASME. Journal of Heat Transfer 96 (1974) 178-183 .
- [13] E. M. Sparrow, H. S. Yu, Local nonsimilarity thermal boundary-layer solutions, ASME. J. Heat Transfer. 93 (1971) 328-332 .
- [14] S. S. Motsa, S. Shateyi, Successive Linearisation Solution of Free Convection Non-Darcy Flow with Heat and Mass Transfer, Advanced topics in mass transfer. 19 (2006) 425-438.
- [15] F. G. Awad, P. Sibanda, S. S. Motsa, O. D. Makinde, Convection from an inverted cone in a porous medium with cross-diffusion effects, Computers and Mathematics with Applications. 61 (2011) 1431-1441.
- [16] C. Canuto, M. Y. Hussaini, A. Quarteroni, T. A. Zang, Spectral Methods Fundamentals in Single Domains, Springer Verlag (2006).